Editors' Suggestion

Transfer reaction products in the ^{40}Ar + ^{232}Th reaction*

Fang Guan (管芳)[1,2] Zhi-Yuan Zhang (张志远)[2,3†] Zai-Guo Gan (甘再国)[2,3,4] Ming-Ming Zhang (张明明)[2]
Jian-Guo Wang (王建国)[2] Ming-Hui Huang (黄明辉)[2,3,4] Long Ma (马龙)[2,4] Hua-Bin Yang (杨华彬)[2]
Chun-Li Yang (杨春莉)[2] Yun-Hua Qiang (强赟华)[2] Xiao-Lei Wu (吴晓蕾)[2] Yu-Lin Tian (田玉林)[2,4]
Jun-Ying Wang (王均英)[2] Yong-Sheng Wang (王永生)[2,4] Su-Yang Xu (徐苏扬)[2,3] Zhen Zhao (赵圳)[2,3]
Xin-Yuan Huang (黄鑫源)[2,3] Zong-Chi Li (李宗池)[2,3] Gang Xie (谢港)[2,3] Lin Zhu (祝霖)[2,3]
Lu-Chong Sun (孙路冲)[1,2,5] Hao Zhou (周浩)[2,3] Xu Zhang (张旭)[2,3]
Jia-Hui Zheng (郑佳卉)[2,3] Hou-Bing Zhou (周厚兵)[1,6‡]

[1]Department of Physics, Guangxi Normal University, Guilin 541004, China
[2]State Key Laboratory of Heavy Ion Science and Technology, Institute of Modern Physics, Chinese Academy of Sciences, Lanzhou 730000, China
[3]School of Nuclear Science and Technology, University of Chinese Academy of Sciences, Beijing 100049, China
[4]Advanced Energy Science and Technology Guangdong Laboratory, Huizhou 516029, China
[5]School of Space Science and Technology, Shandong University, Weihai 264209, China
[6]Guangxi Key Laboratory of Nuclear Physics and Technology, Guangxi Normal University, Guilin 541004, China

Abstract: The distribution of nuclei produced in the ^{40}Ar + ^{232}Th reaction has been studied at the gas-filled recoil separator (SHANS2) at the China Accelerator Facility for Superheavy Elements (CAFE2). The bombardment was carried out at a beam energy of 205 MeV with the detection system installed at the focal plane. Forty-four isotopes heavier than ^{208}Pb were observed. These isotopes were identified as the transfer reaction (or target-like) products, and their relative cross-sections were extracted. Based on the mass distribution of these products, we exclude the possibility that they were produced by fusion-fission reactions; thus, they may originate from quasi-fission of the ^{40}Ar + ^{232}Th reaction.

Keywords: transfer reaction, relative cross sections, quasi-fission, gas-filled recoil separator

DOI: 10.1088/1674-1137/adcb96 **CSTR:** 32044.14.ChinesePhysicsC.49074004

I. INTRODUCTION

Atomic nuclei, composed of protons and neutrons, are many-body quantum systems. When atomic nuclei deviate from the stability line and approach the drip-line region, a range of phenomena distinct from stable nuclei [1] are exhibited, e.g., halo and cluster structures [2], soft excitation modes [3], and shape coexistence [4]. Therefore, studying the exotic properties of unstable isotopes is of significant importance for exploring the limits of atomic nuclei in terms of their proton number and mass, as well as for testing and refining existing nuclear theories. Nuclear reactions are the only method to produce unstable atomic nuclei. For superheavy elements with $Z > 103$, their reaction cross-sections can reach the picobarn (pb) range or even lower [5]. In this case, an optimized high-sensitivity experimental technique is required. In 2021, the Institute of Modern Physics, Chinese Academy of Sciences (IMP-CAS) completed the construction of the China Accelerator Facility for Superheavy Elements (CAFE2). The facility is capable of producing high-intensity heavy-ion beams [6, 7], which enables the experimental study of heavy and superheavy nuclides with extremely low cross-sections.

However, theoretical model calculations indicate that at energies close to the Coulomb barrier, the multi-nucleon transfer reaction [8] is superior to other reactions for the production of certain heavy and superheavy isotopes [9, 10]. Since the 1970s, several experimental studies have been conducted on multi-nucleon transfer reactions

Received 1 February 2025; Accepted 10 April 2025; Published online 11 April 2025

* Supported by the Gansu Key Project of Science and Technology (23ZDGA014), the National Key R&D Program of China (2023YFA1606500), the Guangdong Major Project of Basic and Applied Basic Research (2021B0301030006), the CAS Project for Young Scientists in Basic Research (YSBR-002), the Youth Innovation Promotion Association of the Chinese Academy of Sciences (2023439, 2020409), the National Natural Science Foundation of China (12365016), the National Key Research and Development Program of China (2024YFE0110400, W2412040) and the Natural Science Foundation of Guangxi (2023GXNSFAA026016)

† E-mail: zhangzy@impcas.ac.cn
‡ E-mail: zhb@gxnu.edu.cn

in heavy systems at Coulomb barrier energies, aiming to produce heavy nuclei [11−14]. Recently, the ^{48}Ca + ^{248}Cm [15, 16] and ^{50}Ti + ^{249}Cf [17] reactions were investigated using the velocity filter SHIP and gas-filled recoil separator TASCA at GSI Darmstadt, respectively, and the resulting transfer products were extensively studied. Nevertheless, the exceedingly low cross-sections of superheavy isotopes pose substantial challenges. Efficient separation and detection techniques, similar to the single-atom identification methods employed in the fusion-evaporation reactions of superheavy elements, must be developed to overcome these challenges.

In Ref. [18], the products of the ^{40}Ar + ^{232}Th reaction were detected using a telescope composed of two silicon surface-barrier detectors. The energy spectrum, angular distribution, and cross-sections of products with atomic number $5 \le Z \le 20$ were measured. In this work, we report the study of the ^{40}Ar + ^{232}Th reaction performed at the gas-filled recoil separator SHANS2 at CAFE2 [19, 20]. During the offline analysis, recoil nuclei with atomic number $84 \le Z \le 90$ were identified, and their relative cross-sections and implanted energies were extracted using the method of position-time-energy correlations (recoil implantations (RI) $-\alpha_1-\alpha_2$). However, no decay events from complete fusion reaction products were observed in the experiment. Based on the mass distribution of the recoiling products, the possibility of their formation via fusion-fission reactions was excluded. Thus, the detected recoils in the experiment mainly originated from quasi-fission [21] or multi-nucleon transfer reactions, which are also referred to as incomplete fusion products. The data obtained in this study provide new information for SHANS2 and may serve as a reference for the synthesis of new superheavy nuclides.

II. EXPERIMENTAL DETAILS

The experiment was performed at SHANS2, which is located at CAFE2 at the Institute of Modern Physics in Lanzhou, China. The continuous ^{40}Ar^{12+} beam was provided by the Electron Cyclotron Resonance Ion Source (ECRIS) and was accelerated in the superconducting linear accelerator. The beam particles were accelerated at an energy of 205 MeV, with a beam dose of 1.7×10^{18} and effective irradiation time of 81 h. The beam intensity was approximately 1 pμA.

Four arc-shaped ^{232}Th targets were prepared by electro-deposition onto a 2-μm-thick titanium foil, resulting in an average target thickness of 613 μg/cm^2. These segments were evenly mounted on the edge of a rotating wheel with a diameter of 48 mm, which rotated at approximately 3000 rpm during the irradiation process.

In the experiment, SHANS2 was filled with 1 mbar helium gas as the working gas, and the magnetic rigidity was set to 2.208 T·m. After the separation, the recoiled products were first passed through two multi-wire proportional counters (MWPCs) and subsequently implanted into a double-sided silicon detector (DSSD), which had a thickness of 300 μm and sensitive area of 128 × 48 mm^2. The silicon strip width of the DSSD was 1 mm, forming a total of 6144 pixels. MWPCs were primarily utilized to distinguish between implanted and decay events on the DSSD. The working gas was isobutane, and the optimal working pressure was approximately 300 Pa. As a stopping detector, the DSSD was primarily used to measure implanted signals, α-decay events, and fission event signals. Six side silicon detectors (SSDs), with a thickness of 500 μm and sensitive area of 120 × 63 mm^2, were arranged in a tunnel shape on the front side of the DSSD to detect α-particles and fission fragments that escaped from the DSSD. The overall detection efficiency of the detection system for α-particles emitted from implanted nuclei was measured to be 86(8)%, with approximately 55% contributed by DSSD. All silicon detectors were manufactured by Micron Semiconductor Ltd. Additionally, to register light punching-through particles, three silicon detectors were placed in parallel directly behind the DSSD, each being 300 μm thick, with a sensitive area of 50 × 50 mm^2. An alcohol cooling system was used to cool the silicon-box detector to approximately –25 °C to maintain the energy resolution of the silicon detector. For 5−9 MeV full-energy α-decay events, the energy resolution of the DSSD placed in the focal plane was approximately 30 keV (FWHM), while that for reconstructed α-decay events was 80 keV (FWHM). All signals were shaped by the preamplifier and acquired by a 14-bit self-triggering analog-to-digital converter operating at a sampling rate of 100 MHz. Comprehensive details regarding SHANS2 and the detection system are provided in Ref. [19].

III. RESULTS AND DISCUSSION

In this experiment, an energy-position-time correlation method was employed for identifying isotopes through the analysis of known α-decay energies and half-lives of the nuclei. The energy spectrum of α-like events recorded by the DSSD after the anti-coincidence of the MWPCs is presented in Fig. 1(a). All significant peaks with high statistics were identified through their α-particle energies and half-lives. Fig. 1(b) presents the energy spectrum of α-particles associated with the RI $-\alpha_1$ correlation, with an energy range of $E_{\rm RI}$ = 5 − 9.5 MeV and search time window of Δt (RI $-\alpha_1$) < 100 s. For products with relatively high yields, the identification was further confirmed by comparing the experimental values of α-energies and half-life with those reported in the literature.

RI $-\alpha_1-\alpha_2$ correlation was performed to identify isotopes with low yields. Fig. 1(c) displayed the two-dimensional spectrum of parent and daughter α-particles

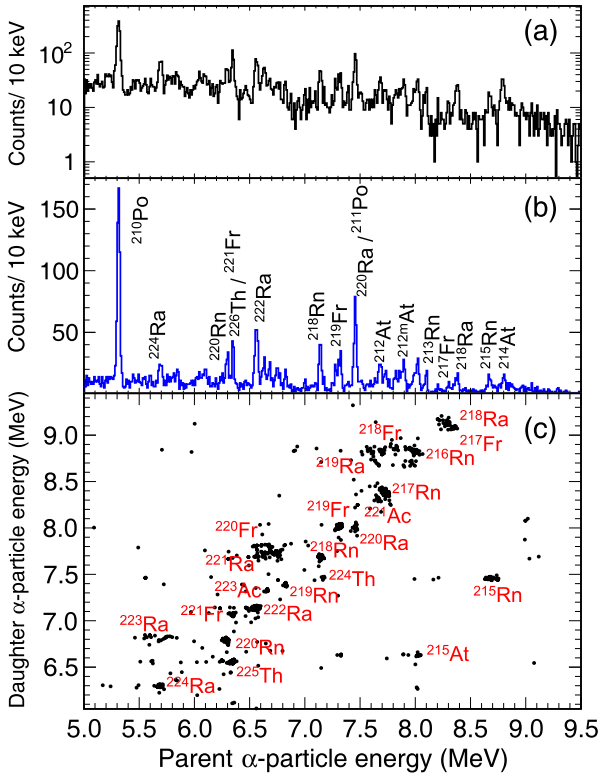

Fig. 1. (color online) (a) α-decay spectrum of all particles detected in the 5−9.5 MeV range for the ^{40}Ar + ^{232}Th reaction in the experiment. (b) α-decay spectrum of the parent nucleus under RI − α_1 correlation, with search time Δt_1 < 100 s. (c) Two-dimensional spectrum of parent and daughter α-particle under the RI − α_1 − α_2 correlation, with search times Δt_1 < 100 s and Δt_2 < 10 s.

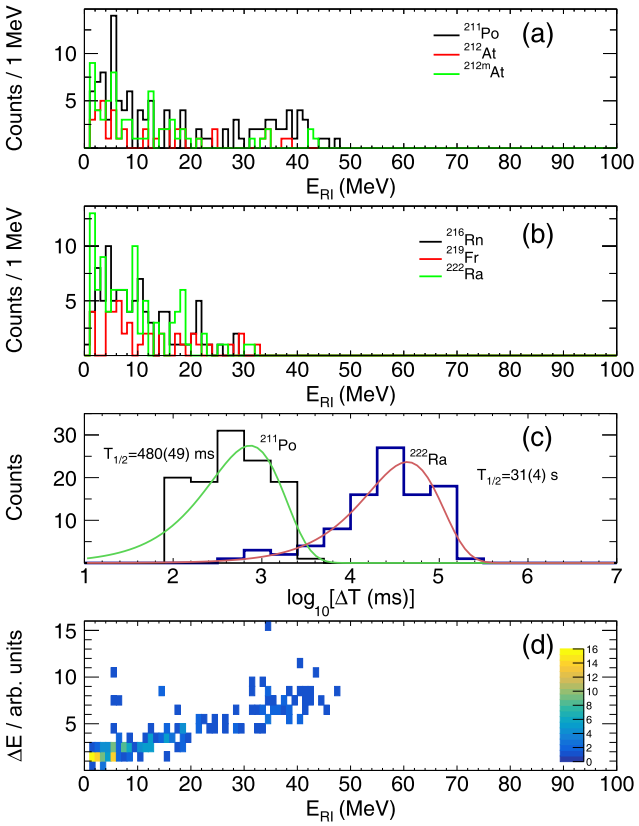

Fig. 2. (color online) (a) Energy distributions of the implanted ^{211}Po, ^{212}At, and ^{212m}At in the silicon box. (b) Energy distributions of the implanted ^{216}Rn, ^{219}Fr, and ^{222}Ra in the silicon box. (c) Half-lives of ^{222}Ra and ^{211}Po measured experimentally. (d) Energy losses of ^{211}Po, ^{212}At, and ^{212m}At under MWPCs vs recoil energy.

under the RI − α_1 − α_2 correlation, with search time windows of Δt (RI − α_1) < 100 s and Δt (α_1 − α_2) < 10 s. A total of 44 isotopes, with mass numbers ranging from 210 ≤ A ≤ 226 and atomic numbers between 84 ≤ Z ≤ 90, were identified. Among these isotopes, 36 were directly implanted.

Fig. 2(a) and (b) show the implanted energy spectra of ^{211}Po, ^{212}At, and ^{212m}At, along with those of ^{216}Rn, ^{219}Fr, and ^{222}Ra. It is noteworthy that, compared to the energy distribution of implanted nuclei reported in Ref. [17], the energy distribution of implanted nuclei in this experiment is primarily concentrated in the region where 1 MeV < E_{RI} < 60 MeV. Only three nuclides, ^{211}Po, ^{212}At, and ^{212m}At, demonstrated both high (HEC, 30 MeV < E_{RI} < 60 MeV) and low (LEC,1 MeV < E_{RI} < 30 MeV) energy components, while the other products only displayed LEC. In Ref. [17], all the implantations show the HEC and LEC for the recoil energy distributions.

Fig. 2(c) presents the time distribution of implantation events for the LEC and HEC of ^{211}Po, as well as the LEC implantation events for ^{222}Ra. The deduced half-lives of ^{211}Po ($T_{1/2}$ = 480(49) ms) and ^{222}Ra ($T_{1/2}$ = 31(4) s) were consistent with the values reported in the literature [22, 23], further confirming the reliability of the experiment. Fig. 2(d) illustrates the relationship between the energy losses of ^{211}Po, ^{212}At, and ^{212m}At in the MWPCs and their implantation energies. Consistent with the observations reported in Ref. [17], significant differences in the energy losses of HEC and LEC in the MWPCs were observed, further supporting the conclusion that the implantation energies consist of two distinct components.

Due to the unknown transmission efficiency ε of transfer reaction products through SHANS2, the absolute reaction cross-sections of the identified nuclides cannot be determined. To obtain an approximate value, the product of the transmission efficiency and cross-sections, $\sigma\varepsilon$, was used as the relative reaction cross sections for the transfer reaction products. In the calculation, the detection efficiency for full-energy α particles in the DSSD was 55%. The relative cross sections for transfer reaction products with half-lives on the order of seconds or less are presented in the Table 1. In Fig. 3, the $\sigma\varepsilon$ of the three isotopic chains, Rn, Fr, and Ra, are compared, and the yields of these isotopes do not vary significantly as the

Table 1. α-decay properties of the transfer reaction products produced in the ^{40}Ar + ^{232}Th reaction. The second and third columns list the α-particle energies and half-lives of these isotopes measured in this work, respectively. The fourth column presents the relative cross-sections of the corresponding isotopes. The fifth and sixth columns provide the corresponding values from the literature.

Isotopes	This work			Literature data		
	E_α/keV	$T_{1/2}$	$\sigma\varepsilon$/pb	E_α/keV	$T_{1/2}$	Ref.
^{211}Po	7456(13)	0.48(5) s	79(22)	7450.3(5)	0.16(3) s	[22]
^{212}At	7679(10)	0.43(10) s	28(9)	7669.3(2)	0.314(2) s	[24]
^{212m}At	7829(10),7879(12)	0.12(2) s	45(14)	7826.7(2),7888.0(2)	0.119(3) s	[24]
^{215}At	8025(13)	0.07(2) ms	15(6)	8026(4)	0.10(2) ms	[25]
^{213}Rn	8094(10)	17.5(30) ms	29(9)	8089(3)	19.5(1) ms	[26]
^{215}Rn	8673(11)	2.6(4)μs	37(11)	8674(8)	2.30(10) μs	[25]
^{216}Rn	8022(13)	44.4(50)μs	63(18)	8050(10)	45(5) μs	[27]
^{217}Rn	7728(12)	0.5(1) ms	44(15)	7738(3)	0.59(6) ms	[28]
^{218}Rn	7140(10)	28(6) ms	50(17)	7129(2)	33.75(15) ms	[29]
^{219}Rn	6824(11)	6.9(15) s	21(8)	6819.1(3)	3.96(1) s	[30]
^{220}Rn	6293(10)	56.5(110) s	68(22)	6288.1(1)	55.6(1) s	[31]
^{216}Fr	9034(22)	2.0(6) μs	8(4)	9004(5)	0.70(2) μs	[27]
^{218}Fr	7606(15),7690(12),7819(11)	29.5(60) ms	48(16)	7616(4),7681(4),7809(5)	21.9(5) ms	[29]
^{219}Fr	7320(10)	28(4) ms	55(18)	7312(2)	20(2) ms	[30]
^{220}Fr	6683(11)	31.3(50) s	39(14)	6677(4)	27.4(3) s	[31]
^{217}Ra	9006(36)	2.3(9) μs	3(2)	8992(8)	1.6(2) μs	[28]
^{219}Ra	7651(21),7940(20)	8.5(15) ms	21(8)	7678(3),7988(3)	10(3) ms	[30]
^{220}Ra	7465(11)	18.2(39) ms	22(8)	7453(7)	18(2) ms	[31]
^{221}Ra	6752(12)	23(4) s	83(27)	6754(5)	28(2) s	[32]
^{222}Ra	6561(10)	31(4) s	124(39)	6558(5)	33.6(4) s	[23]
^{224}Th	7170(17)	0.55(17) s	8(4)	7170(10)	1.05(2) s	[31]

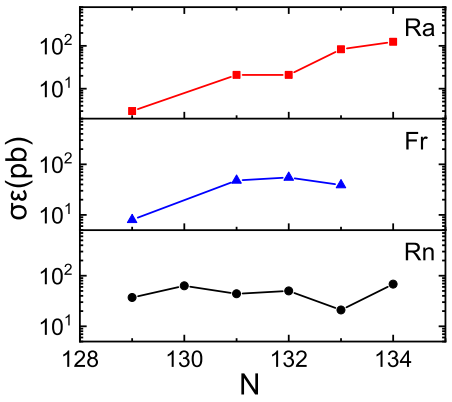

Fig. 3. (color online) Variation of the product of the cross-section and efficiency ($\sigma\varepsilon$) for the implanted Rn, Fr, and Ra isotopes as a function of neutron number (N) in the ^{40}Ar + ^{232}Th reaction.

number of neutrons increases.

To study the generation of these transfer reaction products, two experiments were also conducted, namely for ^{40}Ar + ^{209}Bi and ^{54}Cr + ^{232}Th. The beam energy of the former was 221 MeV, the target thickness was 60 μg/cm^2 C + 500 μg/cm^2 ^{209}Bi, and the beam dose was 2 × 10^{18}. For the latter, the beam energy was 312.1 MeV, the target thickness was 722 μg/cm^2, and the beam dose was 1.7 × 10^{18}.

The distribution of transfer reaction products from both reactions was obtained using the same data processing method. Fig. 4(a) presents a comparison of the product distributions of the ^{40}Ar + ^{232}Th and ^{40}Ar + ^{209}Bi reactions. Although some differences exist (the distribution of isotopes along the N and Z axes is relatively wider in the present data), a large overlap was observed in the isotopic distributions of the two reactions. Fig. 4(b) presents a comparison of the nuclide produced in the ^{40}Ar + ^{232}Th and ^{54}Cr + ^{232}Th reactions, showing a near overlap in the nuclides produced in both experiments.

For the ^{40}Ar + ^{232}Th reaction, the observed isotopes originated from a process in which a large number of nucleons were transferred from the target nucleus to the projectile nucleus. In contrast, in the ^{40}Ar + ^{209}Bi reaction, a significant number of nucleons were transferred

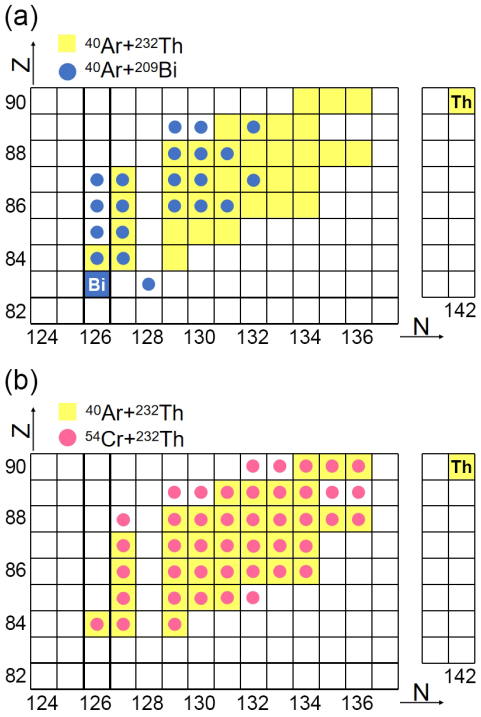

Fig. 4. (color online) Comparison of the distributions of isotopes produced in the ^{40}Ar + ^{232}Th (yellow) reaction with those produced in the ^{40}Ar + ^{209}Bi (blue circles) and ^{54}Cr + ^{232}Th (red circles) reactions.

from the projectile nucleus to the target nucleus. A possible reason for this is that in the ^{40}Ar + ^{232}Th reaction, the nucleon flow tends towards mass and charge symmetry of the system, which is associated with the positive Q-value. Conversely, the ^{40}Ar + ^{209}Bi reaction exhibited the opposite trend, highlighting the influence of Q-values on nucleon flow behavior. The nuclides observed in the ^{40}Ar + ^{232}Th and ^{54}Cr + ^{232}Th reactions were produced by the loss of nucleons from the target nucleus. A comparison of the product distributions indicates that the transfer reaction products of the same target nucleus are largely independent of the projectile type. The results of these experiments are generally consistent with those obtained for ^{50}Ti + ^{249}Cf [17] conducted at TASCA, but the distribution is narrower than that observed in ^{48}Ca + ^{248}Cm [15, 16] performed at SHIP. This may be attributed to the fact that the SHIP device employs velocity for separation of recoil ions, which is better suited to low-yield transfer reaction products.

In addition, because the mass distribution of ^{40}Ar + ^{232}Th reaction products is $A = 210 - 226$ and the product of the charge numbers of the projectile and target nuclei (Z_pZ_t = 1620) exceeds the lower limit (approximately 1600) [33], the quasi-fission (QF) process is expected to begin after this critical value. Therefore, it is speculated that the transfer reaction products observed in this work may originate from the QF process.

IV. SUMMARY

A study of the ^{40}Ar + ^{232}Th reaction was performed at CAFE2 using SHANS2. The relative cross-sections and implanted energies of the recoil products were extracted using the method of position-time-energy correlations. The results demonstrate that the newly constructed gas-filled recoil separator can be utilized to investigate transfer reaction mechanisms. Consequently, SHANS2 is suitable for the synthesis of exotic nuclei from reaction channels other than fusion-evaporation. Based on the substantial nucleon flow populating the isotopes located "northeast" of ^{208}Pb, a possible origin of the identified recoiling products was suggested to be quasi-fission process. The results of the present work can potentially elucidate the different reaction mechanisms, which is helpful for synthesizing new superheavy elements and nuclides.

ACKNOWLEDGMENTS

The authors would like to express their thanks to the accelerator crew and the ion source group of CAFE2 for providing the stable $^{40}Ar^{12+}$ beam.

References

[1] S. G. Zhou, arXiv: 1703.09045
[2] I. Tanihata, H. Savajols, and R. Kanungo, Prog. Part. and Nucl. Phys. **68**, 215 (2013)
[3] C. A. Bertulani, Phys. Rev. C **75**, 024606 (2007)
[4] A. Andreyev, M. Huyse, P. Van Duppen *et al.*, Nature **405**, 430 (2000)
[5] L. C. Sun, Z. Y. Zhang, Z. G. Gan *et al.*, Phys. Rev. C **110**, 014319 (2024)
[6] L. Gong, Z. Wang, W. Dou *et al.*, Nucl. Instrum. Methods Phys. Res., Sect. A **1058**, 168819 (2024)
[7] W. Lu, H. Y. Ma, C. Qian *et al.*, Nucl. Instrum. Methods Phys. Res., Sect. A **1062**, 169207 (2024)
[8] V. I. Zagrebaev and W. Greiner, Phys. Rev. C **83**, 044618 (2011)
[9] G. G. Adamian, N. V. Antonenko, V. V. Sargsyan *et al.*, Phys. Rev. C **81**, 057602 (2010)
[10] V. Zagrebaev and W. Greiner, Phys. Rev. Lett. **101**, 122701 (2008)
[11] H. Freiesleben, K. D. Hildenbrand, F. Pfihlhofer *et al.*, Z. Physik A. **292**, 171 (1979)
[12] M. Schädel, W. Brüchle, H. Gäggeler *et al.*, Phys. Rev. Lett. **48**, 852 (1982)
[13] H. Gäggeler, W. Brüchle, M. Brügger *et al.*, Phys. Rev. C **33**, 1983 (1986)
[14] A. Türler, H. R. von Gunten, J. D. Leyba *et al.*, Phys. Rev. C **46**, 1364 (1992)
[15] H. M. Devaraja, S. Heinz, O. Beliuskina *et al.*, Phys. Lett. B

748, 199 (2015)
[16] S. Heinz, H. Devaraja, O. Beliuskina *et al.*, Eur. Phys. J. A **52**, 1 (2016)
[17] A. Di Nitto, J. Khuyagbaatar, D. Ackermann *et al.*, Phys. Lett. B **784**, 199 (2018)
[18] A. Artukh, G. Gridnev, V. Mikheev *et al.*, Nucl. Phys. A **215**, 91 (1973)
[19] S. Xu, Z. Zhang, Z. Gan *et al.*, Nucl. Instrum. Methods Phys. Res., Sect. A **1050**, 168113 (2023)
[20] L. Sheng, Q. Hu, H. Jia *et al.*, Nucl. Instrum. Methods Phys. Res., Sect. A **1004**, 165348 (2021)
[21] J. Tōke, R. Bock, G. Dai *et al.*, Nucl. Phys. A **440**, 327 (1985)
[22] A. Artna-Cohen, Nucl. Data Sheets **63**, 79 (1991)
[23] S. Singh, A. Jain, and J. K. Tuli, Nucl. Data Sheets **112**, 2851 (2011)
[24] A. Artna-Cohen, Nucl. Data Sheets **66**, 171 (1992)
[25] B. Singh, G. Mukherjee, D. Abriola *et al.*, Nucl. Data Sheets **114**, 2023 (2013)
[26] M. Basunia, Nucl. Data Sheets **108**, 633 (2007)
[27] S. C. Wu, Nucl. Data Sheets **108**, 1057 (2007)
[28] F. Kondev, E. McCutchan, B. Singh *et al.*, Nucl. Data Sheets **147**, 382 (2018)
[29] B. Singh, M. Basunia, M. Martin *et al.*, Nucl. Data Sheets **160**, 405 (2019)
[30] B. Singh, G. Mukherjee, S. Basu *et al.*, Nucl. Data Sheets **175**, 150 (2021)
[31] E. Browne and J. Tuli, Nucl. Data Sheets **112**, 1115 (2011)
[32] A. Kumar Jain, S. Singh, S. Kumar *et al.*, Nucl. Data Sheets **108**, 883 (2007)
[33] M. Itkis, E. Vardaci, I. Itkis *et al.*, Nucl. Phys. A **944**, 204 (2015)